J Bioenerg Biomembr (2012) 44:373–384
DOI 10.1007/s10863-012-9435-2

Light induced transmembrane proton gradient in artificial lipid vesicles reconstituted with photosynthetic reaction centers

Francesco Milano · Massimo Trotta · Márta Dorogi · Béla Fischer · Livia Giotta · Angela Agostiano · Péter Maróti · László Kálmán · László Nagy

Received: 18 December 2011 / Accepted: 19 March 2012 / Published online: 21 April 2012

Abstract Photosynthetic reaction center (RC) is the minimal nanoscopic photoconverter in the photosynthetic membrane that catalyzes the conversion of solar light to energy readily usable for the metabolism of the living organisms. After electronic excitation the energy of light is converted into chemical potential by the generation of a charge separated state accompanied by intraprotein and ultimately transmembrane proton movements. We designed a system which fulfills the minimum structural and functional requirements to investigate the physico/chemical conditions of the processes: RCs were reconstituted in closed lipid vesicles made of selected lipids entrapping a pH sensitive indicator, and electron donors (cytochrome c_2 and $K_4[Fe(CN)_6]$) and acceptors (decylubiquinone) were added to sustain the photocycle. Thanks to the low proton permeability of our preparations, we could show the formation of a transmembrane proton gradient under illumination and low buffering conditions directly by measuring proton-related signals simultaneously inside and outside the vesicles. The effect of selected ionophores such as gramicidin, nigericin and valinomycin was used to gain more information on the transmembrane proton gradient driven by the RC photochemistry.

Keywords Reaction centers · Proton motive force · Ionophores · Pyranine

F. Milano · M. Trotta (✉)
Institute for Physical and Chemical Processes (IPCF),
Bari division, Italian National Research Council (CNR),
Via Orabona 4,
70126 Bari, Italy
e-mail: m.trotta@ba.ipcf.cnr.it

M. Dorogi · B. Fischer · P. Maróti · L. Nagy
Institute of Medical Physics and Informatics, University of Szeged,
Rerrich B. tér 1,
6720 Szeged, Hungary

L. Giotta
Department of Material Sciences, University of Salento,
Strada per Monteroni,
73100 Lecce, Italy

A. Agostiano
Department of Chemistry, University of Bari,
Via Orabona 4,
70126 Bari, Italy

L. Kálmán
Department of Physics, Concordia University,
Montreal, QC, Canada

Abbreviations

RC	Reaction center
POPC	1-Palmitoyl-2-oleoyl-*sn*-glycero-3-phosphocholine
PE	1,2-Diacyl-sn-glycero-3-phosphoethanolamine
PG	1,2-Diacyl-sn-glycero-3-phosphoglycerol
PI	1,2-Diacyl-sn-glycero-3-phosphoinositol
DMPC	1,2-Dimyristoyl-*sn*-glycero-3-phosphocholine
DPPC	1,2-Dipalmitoyl-*sn*-glycero-3-phosphocholine
CL	Cardiolipin
gly-gly	Glycylglycine
Ch	Cholate
LDAO	N,N-dimethyldodecylamine-N-oxide
OG	Octyl glucoside
pmf	Proton motive force

Introduction

The conversion of light into chemical potential by photosynthesis is one of the basic processes in nature and it was subjected to intensive research, specially, in the last decades. By now, thanks to the extensive efforts of research we have quite solid knowledge about the very first steps of these processes, which take place in the reaction center (RC) protein. Much less is known, however, about the structure and function of this protein in the membrane in vivo and specially, how the light induced redox reactions are coupled to proton translocation processes and, as a consequence, about the energization of the membrane.

The photosynthetic reaction center of purple bacteria undergoes a photocycle resulting in the double reduction and double protonation of the loosely bound lipophilic electron carrier ubiquinone-10 (UQ) upon light absorption and in the presence of the exogenous electron donor cytochrome c_2^{2+} (cyt^{2+}) which is oxidized to cyt^{3+}. The light-generated ubiquinol (UQH_2) leaves the RC and reaches a second redox enzyme, the ubiquinol:cytochrome c oxidoreductase, which catalyzes the reverse reaction, namely the reduction of cyt^{3+} to cyt^{2+} by UQH_2 that is oxidized and releases the protons taken up from the cytoplasm into the periplasm, generating the transmembrane proton-gradient required for the metabolic activities of the cell. For reviews see e.g. (Sebban et al. 1995; Allen and Williams 1998; Okamura et al. 2000; Paddock et al. 2003; Wraight 2004). The pH difference built up by the electron transport across the energy converting membranes plays a central physiological role and has been investigated in the literature intensively. a) The proton motive force (pmf), which is created by the transmembrane proton gradient serves the free energy source for the metabolic processes of the living cells (Blankenship et al. 1995). b) Pmf gives rise to a thermodynamic back-pressure to the light initiated electron transport, that inhibits the charge stabilization in the RC protein (van Rotterdam et al. 2001). c) The different pH on the opposite sites of the membrane has differential regulatory effects on the reaction kinetics of the overall electron transport around the transmembrane protein (Faxen and Brzezinski 2007).

Numerous papers in literature deal with photosynthetic systems reconstituted into lipid vesicles in order to study the pmf generation and its effect on the energization of the membrane using different approaches: Light harvesting complex (LHC) of the photosystem II (PSII) (Wardak et al. 2000), photosystem I (PS I) and ATP-synthesizing complexes (Hauska et al. 1980), RCs of purple bacteria with light harvesting (LHC) complexes (Molenaar et al. 1988) and very recently PS I (Yang et al. 2005) and PS II (Petrova et al. 2011) were also reconstituted into lipid vesicles and their functions were studied.

The redox cycle around the RCs of purple bacteria, which is usually visualized in the literature by the separation of the cytochrome turnover on the donor (outer, periplasmic) side of the membrane and by the quinone cycle on the acceptor (internal, cytoplasmic) side of the membrane (see e.g. (Shinkarev and Wraight 1993)) is a very complex redox and acid/base reaction (Osvath and Maroti 1997; Milano et al. 2007) which is far from complete understanding. The contribution of redox partners, namely the $UQ/UQH_2//cyt^{3+}/cyt^{2+}$ couple to the acid/base change of the RC/vesicular system was demonstrated also by Hellingwerf (Hellingwerf 1987). This author showed the acidification of the outer medium of the reconstituted system mediated by UQ/UQH_2 across the bilayer membrane at very high pH (with the optimum around 9.5).

When isolated RCs are illuminated in the presence of an exogenous electron donor (e.g. cyt^{2+} or ferrocene) and a quinone pool, an alkalization of the medium is measured if the buffering capacity of the solution is kept low. The increase of the pH accompanying the photocycle can easily be followed by the fluorescence of a pH sensitive dye, pyranine, as demonstrated in Triton X-100 micelles (Agostiano et al. 2004). Being a highly charged molecule, pyranine is very suitable for investigating pH changes in liposomal systems (Kano and Fendler 1978; Holoubek et al. 2007; Wiedenmann et al. 2008). It has been used successfully to follow the proton uptake/release in various systems, associated with the function of membrane bound proteins like F_0F_1-ATPase during continuous ATP biosynthesis in lipid coated glucose oxidase (GOD) microcapsules (Duan et al. 2009) as well as during photoinduced quinone reduction catalyzed by the RC (Agostiano et al. 2004).

To model the structure and function of biological membrane, different types of phospholipids (e.g. 1,2-Dimyristoyl-*sn*-glycero-3-phosphocholine (DMPC), 1,2-Dipalmitoyl-*sn*-glycero-3-phosphocholine (DPPC), 1-Palmitoyl-2-oleoyl-*sn*-glycero-3-phosphocholine (POPC), soybean or egg yolk lecithin) were used because phospholipids are major components of the biological membranes (ranging from 25 % to 55 % depending on the types of the membrane) and the structures of the artificial membranes prepared by using these lipids resemble that of the in vivo membrane from many points of view (Lande et al. 1995; Krishnamoorthy and Krishnamoorthy 2001; Brzustowicz et al. 2002; Trotta et al. 2002; Barlic et al. 2004; de Almeida et al. 2005; Gensure et al. 2006; Filizola et al. 2006; Pandit et al. 2007). Besides the zwitterionic POPC, other phospholipids such as 1,2-diacyl-sn-glycero-3-phosphoethanolamine (PE), 1,2-diacyl-sn-glycero-3-phosphoglycerol (PG), cardiolipin (CL) are also very common in the bacterial membranes (Nagy et al. 1999; Donohue et al. 1982; Wood et al. 1965; Steiner et al. 1970; Onishi and Niederman 1982) and proved to have specific functions in the membrane (Pilotelle-Bunner et al. 2009). The role of the cholesterol (or its derivatives) as a major constituent in the artificial membrane is also widely demonstrated (Brzustowicz

et al. 2002; Barlic et al. 2004; de Almeida et al. 2005; Henriksen et al. 2006; Kahya and Schwille 2006).

By using different lipids with different head groups and hydrocarbon side chains we managed to prepare lipid vesicles with relatively low proton conductivity. When pyranine-containing RC-vesicles are illuminated in the presence of suitable donor-acceptor system the internal pH increases, as indicated by the fluorescence signal, and reaches a maximum. When the light is switched off, the fluorescence signal decays due to passive transport of protons across the bilayer. The permeability of the bilayer to different ions has been modulated by the addition of suitable ionophores. The resulting time-course of the light-induced membrane energization will be shown and discussed.

Materials and methods

Cell culturing and protein purifications Rb. sphaeroides R-26 cells were grown photoheterotrophically under anaerobic conditions. RCs were prepared by N,N-dimethyldodecylamine-N-oxide (LDAO) solubilization followed by ammonium sulfate precipitation and DEAE Sephacel anion exchange chromatography (Tandori et al. 1995).

Liposome and proteoliposome preparation Throughout the paper vesicles containing RC are called proteoliposomes to distinguish them from pure lipid liposomes. Liposomes were prepared by a gel filtration micelle-to-vesicle transition technique. The appropriate amounts of phospholipids (POPC, PG) and cholesterol are dissolved in chloroform and dried on the wall of a conical tube under a nitrogen stream forming a thin film. In all experiments 4 mg POPC are used and throughout the paper the bilayer composition is given in molar ratio with respect to this amount of POPC. The film is dissolved with 0.5 ml of 1.4 % cholate (Ch) or 4 % octyl glucoside (OG) in phosphate buffer (10 μM potassium phosphate, 10 mM KCl, 1 mM pyranine, pH 7.2). The solution is sonicated in ice with the titanium probe of Branson sonifier Mod. 250 (10 shots, output power is about 25 W, duty cycle 40 %) to form clear mixed phospholipid/detergent micelles. For proteoliposomes preparation, a small volume of the RC solution is added at this stage and vigorously shaken to allow the phospholipid/protein/detergent micelles formation. The solution is then loaded on a 20 cm Sephadex G-50 superfine gel filtration column (exclusion limit 8–10 kDa), previously equilibrated with phosphate buffer (10 μM potassium phosphate, 10 mM KCl, 1 mM pyranine, pH 7.2). Effective removal of the detergent during column elution (Milano et al. 2009) resulted in the formation of vesicles that were collected and loaded on a second column equilibrated with pyranine-free buffer (10 μM potassium phosphate, 16 mM KCl, pH 7.2) in order to remove the external pyranine (Trotta et al. 2002). The KCl concentration is increased from 10 to 16 mM in order to make the solutions with and without pyranine isotonic.

Fluorescence measurements Pyranine is a water-soluble fluorescent dye whose fluorescence yield is very sensitive to pH in the interval close to the $pK_a = 7.2$ of the ionization of the hydroxyl group of the molecule in aqueous solution. The ratio of fluorescence at 510 nm between the excitation peaks excited at 405 nm and 465 nm can be calibrated and used as an internal pH indicator regardless the absolute value of the emission intensity (Kano and Fendler 1978; Wiedenmann et al. 2008). This allows us to estimate the initial and final pH values in the vesicles. The steady state fluorescence excitation spectra and kinetic traces were measured by a Perkin Elmer MPF 44-A spectrofluorimeter, which was supplied with a homemade sample holder assuring quick and continuous stirring during pH adjustment and chemical treatment. The RC photocycle was driven by a 150 W projector lamp whose light was directed to the side wall of the cuvette with a light guide and filtered with a red filter in order to minimize the light induced photolysis of $[Fe(CN)_6]^{4-}$ which results in an unwanted alkalization of the solution (Deamer and Harang 1990). The signal of the spectrofluorimeter was fed to one of the channels of an USB analog/digital converter (Picoscope 2203) connected to PC for storing and analyzing.

pH measurements In order to measure the light induced pH changes simultaneously outside and inside the vesicles a pH electrode was immersed in some experiments in the reaction mixture placed in a spectroscopic cuvette containing a stirrer bar and its signal was connected to the second channel of the Picoscope.

Fluorescence microscopy Pyranine-containing liposomes were diluted by phosphate buffer pH 7.0 as needed and cast on a microscopy glass. Fluorescence images were recorded using an epifluorescence microscope (Axiomat, Zeiss, Germany) with excitation at 450–490 nm, emission at 515 nm and a magnification factor of 50-fold.

All the chemicals for bacteria culturing, RC extraction and purification, vesicles preparation and photochemical measurements were purchased from Sigma and Molar Chemicals Ltd and used without further purification.

Results and discussion

Vesicles prepared by gel filtration micelle-to-vesicle transition technique showed an elevated proton permeability that did not allow the establishment of permanent proton

gradient across the bilayer. We have improved the protocol for both liposomes and proteoliposomes preparation with entrapped pyranine and low buffering capacity, which showed a rather high degree of impermeability to proton diffusion across the bilayer. Proteoliposomes prepared by this protocol can be used to investigate the photoinduced proton translocation across the lipid bilayer.

Liposomes

In order to demonstrate the effective entrapment of pyranine in the internal aqueous compartment of the liposomes, a fluorescence micrograph has been taken. The concentrated sample showed diffuse green fluorescence due to the high liposome concentration that uniformly covered the microscopy glass. Upon dilution, as high as 1000-fold, large aggregates were detected; above this dilution, large numbers of small spots were observed (Fig. 1). It is worthwhile to underline that the green spots are not due to single liposomes, rather to clusters, but it is clearly seen that pyranine still remained within the aggregates.

The response of liposome suspension to the addition of base (100 μM KOH) was checked by measuring the fluorescence of entrapped pyranine at 510 nm with excitation at 465 nm. The percentage of leakage was determined by the ratio of the fluorescence increase upon addition of the base and addition of Triton X-100 that breaks the liposomes and equilibrates the internal and external pH.

Figure 2 shows the kinetic traces of the fluorescence of pyranine entrapped into liposomes of different composition prepared by using Ch or OG.

First, we prepared liposomes either with pure POPC and with a mixture of POPC:cholesterol 5:1 using 1.4 % Ch as solubilizing agent. In the first case the percentage of leaking is very high, 84 % and decreased to 74 % in the presence of cholesterol. The origin of this improvement is discussed later. Second, we used 4 % OG as solubilizing agent and

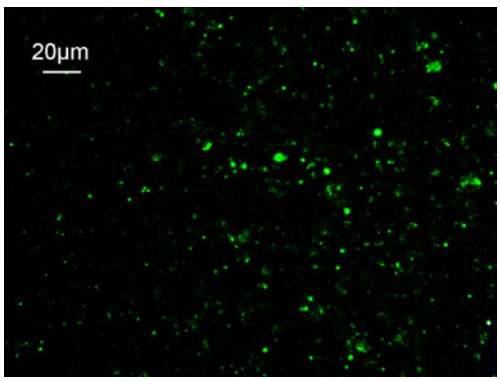

Fig. 1 Fluorescence micrograph of pyranine-containing liposomes at 50× magnification, with excitation at 450–490 nm and emission at 515 nm. The sample was diluted 1:1000

obtained significant improvement of the liposome sealing with a leakage of 57 %. Finally, by adding PG to the lipid mixture the leakage dropped to 37 %. at the final composition of POPC:cholesterol:PG with molar ratios of 5:1:1, respectively. This latter improvement is most likely due to the negative charge of PG, which electrostatically repels the negatively charged pyranine and prevents its association with the liposome surface.

The effect of exchange of Ch by OG is more complicated to understand. The role of some residual detergent molecules concentrated at the interfaces, or at different domains in the bilayer cannot be excluded. Also, the domain formation of the membrane can be different in the presence of different types of detergents. Although traces of detergents are not effective in altering the main phase behavior (e.g. melting temperature) of the lipid (Riegler and Mohwald 1986), it is expected that they can facilitate the proton conductivity across the membrane. One of the possible reasons of the unexpectedly high proton conductivity of the membranes is the presence of traces of contaminants, like weak acids or bases (Gutknecht 1987). Traces of cholate, as solubilizing agent act as weak acid and can compromise the sealing of the vesicles, which is not the case for OG.

Furthermore, the leakage of the liposomes depends on the identity of the chemical added to increase the pH. When exposing the liposomes to a 1 pH unit jump by addition of KOH, glycylglycine (gly-gly) or Tris–HCl (Fig. 3) we observed striking differences: the addition of KOH results in a sudden increase of the pyranine fluorescence, but the result shows that the pH in the internal and external compartments is not completely equilibrated. In the case of the addition of gly-gly the internal pH remained almost unchanged, while upon addition of Tris–HCl the internal and external pH equilibrated within about 100 s. This observation can be explained by the different ionic state of the solutions. With the ionic KOH or gly-gly a transmembrane proton gradient is built up, which is eliminated by breaking the vesicles with TX-100. Anyway, OH^-, like H^+ as well, has a quite high membrane permeability due to its small size and it can cross the bilayer using a special (Grotthuss) mechanism involving water chains always present in the membrane. The best sealing is obtained if the pH is increased by gly-gly which is charged in both protonated and deprotonated form. On the other hand, Tris–HCl can cross the bilayer in its neutral deprotonated form and the inside and outside pH equilibrates by the addition of this buffer. No substantial change can be measured with TX-100 in this case.

Proteoliposomes

When the RC is incorporated in the bilayer at a 1:1000 ratio with respect to POPC, the proton leakage of the

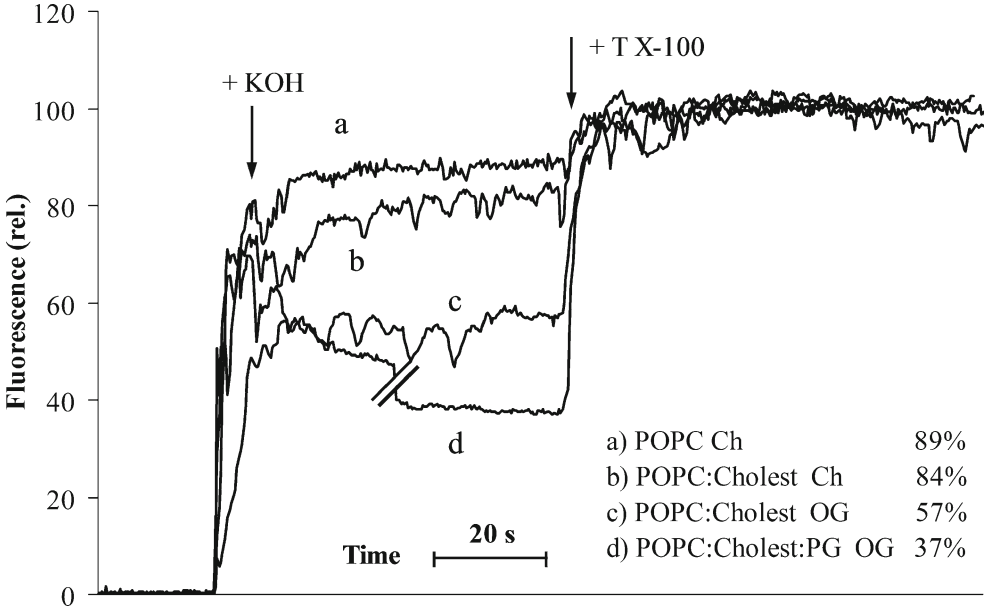

Fig. 2 Kinetics of the pyranine fluorescence entrapped in liposomes prepared from POPC, PG and cholesterol as indicated. The solubilizing detergents were Ch and OG. *Arrows* indicate the addition of KOH (in order to increase the external pH) or TX-100 (to break the liposomes). The numbers in percentage show the degree of leakage that was estimated from the stationary levels of the pyranine fluorescence before and after addition of TX-100. λ_{exc}: 465 nm, λ_{em}: 510 nm

proteoliposome increases (ca 60 %, data not shown). We could obtain better sealing by progressively increasing the cholesterol concentration up to a bilayer composition of POPC:cholesterol:PG 5:5:1 for which a leakage of about 30 % was obtained. Above this cholesterol concentration the proteoliposome suspension becomes too scattering with high tendency to sediment. If PG is substituted with an equal amount of 1,2-Diacyl-sn-glycero-3-phosphoinositol (PI) similar results are obtained. The different proton leakage values for different preparations and measuring conditions are summarized in Table 1.

The method of mixture of membrane proteins with different phospholipids (DMPC, DPPC, POPC, soybean or egg yolk lecithin) is widely used if the structure and function of biological membrane are tried to model. POPC is of special interest, since at around physiological temperature it is in a fluid phase, having the phase transition temperature of −5 °C (Thewalt and Bloom 1992). The effect of high concentration of cholesterol is ambiguous. On one hand, above the melting temperature, it increases the microviscosity. On the other hand it induces the heterogeneity in the distribution of membrane domains and the liquid-disordered L_d and liquid-ordered L_o phases. Although it has been reported that proton permeability correlates weakly with fluidity (Lande et al. 1995), the reports on the effect of the increasing cholesterol concentration on the proton permeability is inconclusive in the literature. It is generally accepted that in PC membranes cholesterol reduces the proton conductivity, probably decreasing the water content and thereby decreasing the probability of formation of the H-bonded water wire across the membrane (Deamer and Nichols 1989; Krishnamoorthy and Krishnamoorthy 2001).

Unfortunately the proton leakage cannot be eliminated completely. Proteins tend to show a certain preference to bind to the boundaries between the immiscible ordered and disordered regions, which could facilitate membrane permeabilization (Barlic et al. 2004). The RC/lipid complexes

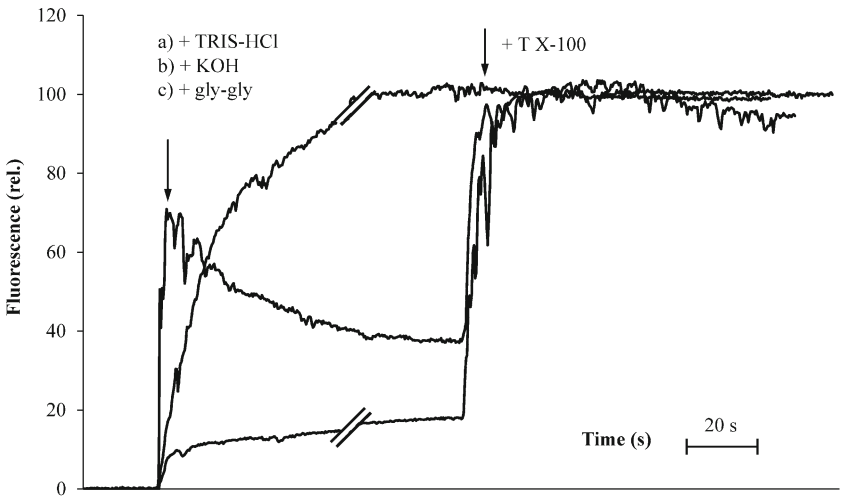

Fig. 3 Kinetics of the pyranine fluorescence of POPC/cholesterol/PG (5:1:1) liposomes, prepared by OG solubilization. KOH, Tris–HCl or glycylglycine and TX-100 was added in order to induce pH change and to break the liposomes, respectively (see the *arrows*). λ_{exc}: 465 nm, λ_{em}: 510 nm

Table 1 The summary of different proton leakage values for different preparations and measuring conditions. Measurement was done as described in Figs. 2 and 3. The mixed micelles were prepared by the detergents cholate or OG, and the pH change was induced by addition of KOH, Tris–HCl or gly-gly as indicated. The leakage values are indicated in percentage of the equilibrium reached after destroying the vesicles by the addition of the detergent TX-100

	Lipid	Cholesterol	Detergent	pH jump	Leakage (%)
Liposomes	POPC	–	Cholate	KOH	84
	POPC	+[a]	Cholate	KOH	74
	POPC	+[a]	OG	KOH	57
	POPC/PG	+[a]	OG	KOH	37
	POPC/PG	+[b]	OG	Tris–HCl	100
	POPC/PG	+[b]	OG	gly-gly	20
Proteoliposomes[d]	POPC/PG	+[b]	OG	gly-gly	60
	POPC/PG	+[c]	OG	gly-gly	30

[a] /POPC:cholesterol = 5:1; [b] /POPC:cholesterol:PG:=5:1:1; [c] /POPC:cholesterol:PG:=5:5:1; [d] /RC:lipid = 1:1000

made by different chain length lipids also indicated that lipid packing defects and differences in membrane thickness at the interfaces might contribute to the redistribution of lipid molecules around the protein and to modify the interaction (Riegler and Mohwald 1986).

The characterization of the proton sealing/conducting capacity of the proteoliposome requires careful determination of the buffering capacity and activity of protons in our systems. This is not an easy task as they are sensitive to the solute constitution and pH: e.g. for example the activity coefficients of H^+ ion (f_{H+}) are 0.33 for 0.03 % Triton X-100, and only 0.12 for 0.04 % dodecylmaltoside (Kalman et al. 1997). Further to the complicated initial conditions of the very heterogeneous lipid/RC system the pH, and consequently the buffering capacity or f_{H+} show a transient change in time. This transient let us to give a good estimate of the pH, however, further investigations are needed to give a more precise quantitative description of the system.

RC photocycle

As already mentioned, when the RC is in the presence of the electron donor cyt^{2+} and the electron acceptor quinone pool, the continuous illumination of the system results in the production of cyt^{3+} and quinol and the alkalization of the solution in low buffer conditions. A result of typical experiment is shown in Fig. 4., where the pyranine fluorescence is recorded as a function of time to monitor pH change associated with the RC photocycle. The proteoliposomes eluted from the second, pyranine-free column, are diluted 1:10 in 10 μM potassium phosphate and 16 mM KCl at pH 7.0. Under these conditions the RC final concentration is typically 0.1–0.2 μM. As electron donor we added 2 μM horse heart cyt c and 1.5 mM $[Fe(CN)_6]^{4-}$. Neither cytochrome c nor $[Fe(CN)_6]^{4-}$ cross the membrane, making the RC function asymmetric since during the photocycle, only the RCs with dimer facing the external solution can operate, and the uptake of protons occurs from

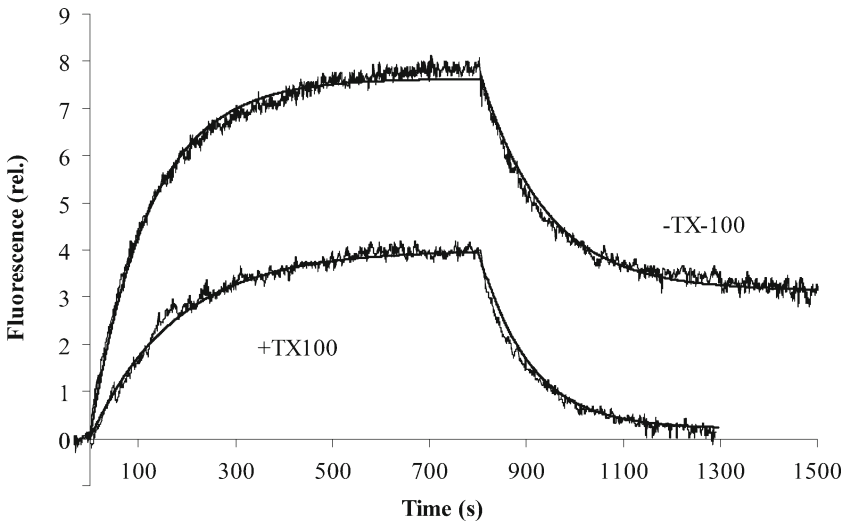

Fig. 4 Kinetics of pyranine fluorescence of POPC/cholesterol/PG (5:5:1) proteoliposomes due to the light induced protonation processes with or without TX-100 (as indicated). Conditions: 0.2 μM RC, 100 μM decylubiquinone, 2 μM cyt c^{2+} and 1.5 mM $[Fe(CN)_6]^{4-}$ were added for keeping the photocycle. λ_{exc}: 465 nm, λ_{em}: 510 nm. *Solid lines* indicate the fitted curves by the parameters summarized in Table 1

the interior of the proteoliposomes. Cyt must be added at the lowest possible concentration since it quenches the pyranine fluorescence and reduces the vesicle stability. The presence of $[Fe(CN)_6]^{4-}$ ensures that the oxidized cytochrome is rapidly re-reduced, so that the reaction can continue without being limited by cyt^{2+} consumption. Also, we checked that the $[Fe(CN)_6]^{4-}$ itself in the absence of cytochrome, cannot drive the photocycle (data are not shown). As electron acceptor, UQ_{10} is not suitable, since it can be added only at the beginning in the mixed micelles during the proteoliposomes preparation and its final concentration can hardly exceed 5 μM. The water soluble analog ubiquinone-0 was also ruled out due to its poor interaction with the Q_B site. Faster and larger photoinduced pH changes were obtained with decylubiquinone (2,3-dimethoxy-5-methyl-6-decyl-1,4-benzoquinone, DQ). This ubiquinone synthetic analog is an exogenous, hydrophobic quinone that has a saturated 10-carbon side chain with a methyl group at the end and can easily penetrate into the liposomal membrane when added as concentrated ethanolic stock solution(Telford et al. 2010). DQ final concentration was typically 50 μM, but was varied in some experiments.

The excitation spectra of the pyranine fluorescence were also measured in different samples and phases of the kinetic transients. When the analysis was carried out it should be considered that the addition of reagents, specially the absorption by the cytochrome Soret band, modified the spectrum of the untreated sample (Fig. 5). This figure shows that the actinic light induced an alkalization inside the proteoliposomes which was partly eliminated by the addition of ionophore (in this case nigericin).

A simple model can be constructed to describe the fluorescence increase in the light and the following dark phases of the transients.

When the light is switched on the alkalization of the internal compartment can be observed due to the RC photochemistry as explained above. However, the existing pH gradient induces passive proton translocation across the membrane, so an increase of the external pH is also expected and the pH gradient can be evidenced only if the photocycle is driven faster than proton leakage, occurring with a rate constant k_{leak}. Another process to be taken into account is the reoxidation (characterized by the rate constant k_{ox}) of dihydroubiquinol (DQH_2) which accumulates during the continuous turnover of the RC under light excitation. DQH_2, together with its oxidized form DQ, can easily cross the membrane and is in interaction with the redox systems in the inner and the outer compartments. Outside of the vesicles the DQH_2 releases the protons after oxidation by the $[Fe(CN)_6]^{3-}/[Fe(CN)_6]^{4-}$// cyt c^{3+}/cyt c^{2+} system. This process itself would result in the acidification of the outer compartment as found by Hellingwerf (Hellingwerf 1987) at very high pH values. However, in our system, the created pH difference in the two sides of the membrane tends to equilibrate due to the proton translocation so we never observed the external acidification. We found that the initial rate of the light reaction is proportional to the light intensity (Table 2), indicating that, at the concentration used, the RC photochemistry is not limited by the turnover rates of the pools on the donor and on the acceptor sides.

The fluorescence change in the light phase after some time reaches a plateau which depends on the light intensity and several opposing processes like proton consumption by the RC photochemistry, proton wiring across the membrane, quinol reoxidation. The resulting trace can be approximated by an exponential rise to maximum according to the equation:

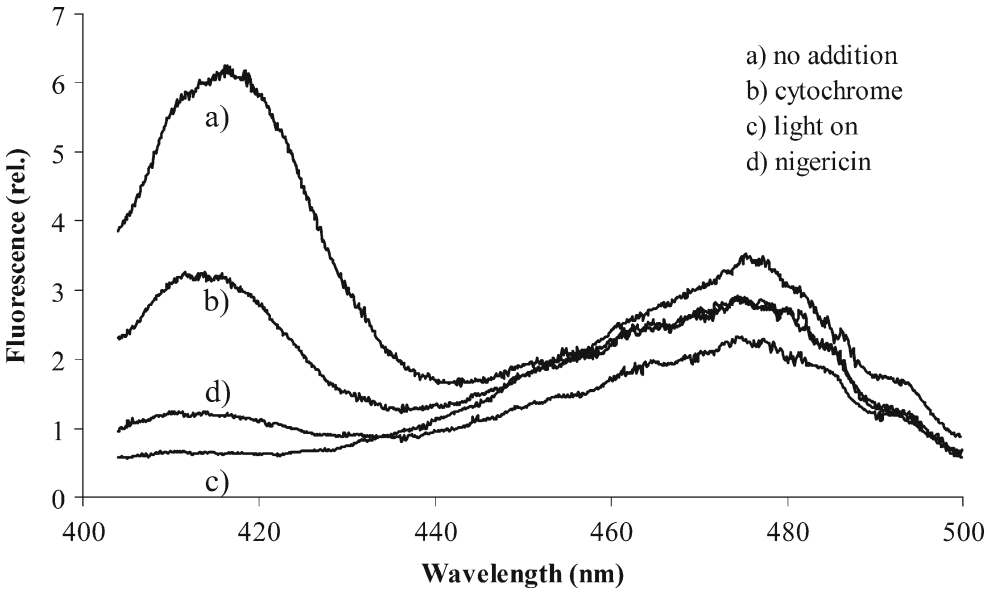

Fig. 5 Fluorescence excitation spectra of different proteoliposome samples measured at 510 nm. "no addition" indicate the sample without addition of reagents, "cytochrome" refers to a sample that was treated by cytochrome c_2, decylubiquinone and $[Fe(CN)_6]^{4-}$ as described in "Materials and methods". "light on" and "nigericin" indicate the spectra measured at the plateau of the light phase without and with ionophore (nigericin in this case), respectively

Table 2 The initial rate of the pyranine fluorescence rises due to pH changes when the RC photochemistry was initiated by light. Transients were measured as shown in Fig. 4 at different light intensities as indicated. The initial rate was calculated as the first derivative of the fitted curves (see details in the text)

Light intensity (W/cm^2)	0.6	1.2	2.2	3.2
Initial slope (s^{-1})	0.016	0.030	0.055	0.089

$$F_{light} = A_{light}\left(1 - e^{-k_{light}\cdot t}\right)$$

where F_{light} is the change in the fluorescence intensity in the light and A_{light} is fluorescence intensity at the plateau and k_{light} is the rate constant.

When the light is switched off the kinetics is changed because the continuous and fast proton consumption by the RC turnover is stopped, so that the fluorescence kinetics will be determined only by the pH changes connected to the quinol reoxidation and to the proton wiring according to the equation:

$$F_{dark} = A_{dark}e^{-k_{dark}\cdot t} + A_{\infty}$$

where F_{dark} is the change in the fluorescence intensity in the dark, A_{dark} is the fluorescence intensity at the end of the light phase, k_{dark} is the rate constant and A_∞ is an additive constant accounting for the non-complete relaxation of the system. It is important to note that k_{dark} is strongly affected by additions of ionophores or detergent. In fact in the dark phase we observe a decay reflecting the slower process, either proton leaking or quinol oxidation. In the absence of ionophores, if the vesicles are sealed enough, we have that $k_{leak} < k_{ox}$, so in this case $k_{dark} \sim k_{leak}$; the constant term A_∞ accounts probably for a population of better sealed vesicles. In the presence of ionophores k_{leak} increases and if the slower process becomes quinol oxidation we can write that $k_{dark} \sim k_{ox}$ and A_∞ becomes also very small. In the presence of the detergent TX-100 0.3 % the vesicular system is broken (Fig. 4). The photocycle can proceed with all RC interacting with cytochrome but the light phase rate is not faster since this high concentration of detergent makes the RC photochemistry less efficient. The dark recovery is faster due to the elimination of the proton wiring process, reflecting only the quinol reoxidation process.

The results of the fitting and the parameters are summarized in Fig. 4 and Table 3, respectively.

Figure 6 shows that the kinetics of both the light and the dark phases of the cycle depend on the quinone concentration as well. If DQ is not added no photocycle can be measured; increasing the DQ concentration more turnovers can be measured (i.e. the amplitude of the fluorescence rise increases) without significant effect on the initial slope of the signal. Additionally, the rate of the dark relaxation phase increases with the quinone concentration.

This latter finding would reflect that this process follows a second order kinetic reaction, in accordance with our earlier studies (Milano et al. 2007) as well. However, a relatively large amount of $[Fe(CN)_6]^{3-}$, a potential quinol oxidant formed after the addition of $[Fe(CN)_6]^{4-}$, is always present in the solution, making the reaction "pseudo-first order", so that the decay will be monoexponential with the rate constant of $k_{ox} \sim k_{dark}$.

The actual generation of a transmembrane proton gradient can be evidenced comparing the kinetics in the presence or absence of ionophores that change the proton redistribution on the two sides of the proteoliposome membrane. When these chemicals are added to the sample in the form of concentrated ethanolic solution (i.e. the small amount of ethanol itself has no effect on the membrane permeability) they are solved relatively rapidly in the membrane and depending on the species they have different effects on the transmembrane proton gradient. The ionophores were added in saturating concentration after the plateau of the light phase is reached while the light was still on. The effects of the different ionophores, gramicidin, nigericin and valinomycin are explained here and the parameters of the kinetic traces are summarized in Table 4.

Gramicidin A This ionophore is a linear pentadecapeptide that forms a channel permeable to most monovalent cations, while excluding divalent cations and anions. When gramicidin was added to the sample the rate of the light reaction decreased from 14.6×10^{-3} s^{-1} to 8.9×10^{-3} s^{-1}, while that of the dark reaction increased (from 4.7×10^{-3} s^{-1} to 6.9×10^{-3} s^{-1}). When this chemical was added at the plateau of

Table 3 Kinetic parameters of pyranine fluorescence transients measured for samples without or with the addition of the detergent TX-100 at a concentration of 0.3 %, as indicated. Transients were measured as shown in the protocol in Fig. 4. k_{light} and k_{dark} are the calculated rates of the fluorescence increase in the light and the decrease in the dark phases, respectively. A_{light}, A_{dark} and A_∞ are the preexponential constants referring to the relative contributions of the components to the fluorescence rise. The maximum error of the measurement was 10 %

	Light phase		Dark phase		
	A_{light}(rel.)	k_{light}($\times10^{-3}$ s^{-1})	A_{dark}(rel.)	k_{dark}($\times10^{-3}$ s^{-1})	A_∞(rel.)
− TX-100	7.6	8.2	4.3	7.4	3.1
+ TX-100	4.0	5.6	3.2	9.6	0.2

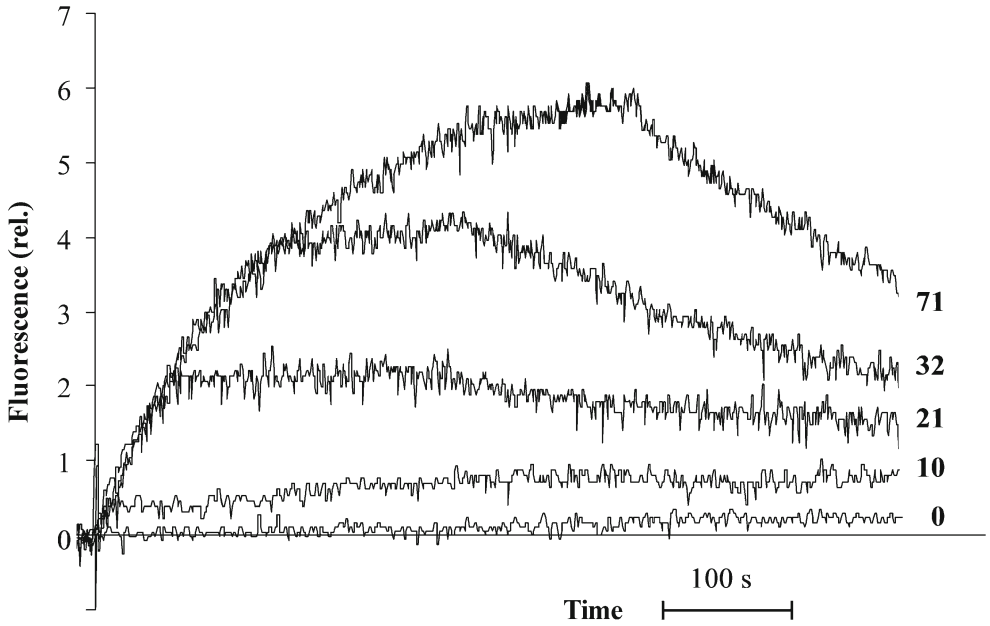

Fig. 6 The effect of the quinone concentration on the time course of pyranine fluorescence. Measuring conditions are same as described in Fig. 4, but different quinone concentrations were applied as indicated by the numbers in terms of μM

the light phase a new equilibrium was reached at the level of about 80 % of the maximum (data are shown later). After switching the light off, the signal decayed with a rate constant k_{dark} = 6.9·×10^{-3} s^{-1}. These findings can be easily explained since, as already mentioned, the traces reflect the simultaneous light-induced proton uptake by the RC and several dark processes among which the passive proton translocation across the membrane and the reoxidation of the quinol. After addition of gramicidin the passive proton flow rate is increased, so that the rate of the light phase decreased and the lower plateau is reached (data are shown later). At the plateau of the light phase, the rates of proton pumping and dark processes are equal giving rise to a steady state. After addition of gramicidin the steady state shifts downwards to a lower pH. For the same reason the dark relaxation is faster in the presence of this chemical, having a constant of 6.9 ×10^{-3} s^{-1} compared to the value of 4.7 × 10^{-3} s^{-1} obtained for the untreated sample.

Nigericin is a well-known representative of naturally polyether ionophore antibiotics. It is able to form pseudo-macrocyclic complexes with mono and divalent cations and transport of the cations across cellular membrane. Most commonly it is an antiporter of H^+ and K^+. The time course of the fluorescence after the addition of nigericin resembles the kinetics of gramicidin with slight differences. The rise time of the fluorescence change slightly increased for the light and decreased for the dark phases (k_{light} = 6.9 × 10^{-3} s^{-1} and k_{dark} = 5.9 ×10^{-3} s^{-1} for the nigericin), respectively.

Valinomycin is a dodecadepsipeptide, made of twelve alternating amino acids and esters to form a macrocyclic molecule. It functions as a potassium-specific transporter and facilitates the movement of K^+ through lipid membranes "down" an electrochemical potential gradient. There is only a moderate effect on the kinetics in the light phase (k_{light} decreased to k_{light} = 9.1 ×10^{-3} s^{-1}) while the dark relaxation

Table 4 Kinetic parameters of pyranine fluorescence transients measured for samples without (No addition) and with ionophores (as indicated). Transients were measured as shown in the protocol in Fig. 4. k_{light} and k_{dark} are the calculated rates of fluorescence increase due to the RC photochemistry and passive proton translocation in the light phase, respectively. Data were calculated according to the equation $F_{light} = A_{light} \cdot \left(1 - \exp\left(-k_{light} \cdot t\right)\right)$ and $F_{dark} = A_{dark} \cdot \exp\left(-k_{dark} \cdot t\right) + A_{\infty}$ for the light and dark phases, respectively and explained in the text. The measuring light intensity was 3 W/cm^2. The maximum error of the measurement was 19 %

	No addition		Gramicidin		Nigericin		Valinomicyn	
	A(rel.)[(a)]	k × ·10^{-3} (s^{-1})[(b)]	A(rel.) [(a)]	k × ·10^{-3} (s^{-1})[(b)]	A(rel.) [(a)]	k × ·10^{-3} (s^{-1})[(b)]	A(rel.) [(a)]	k × ·10^{-3} (s^{-1})[(b)]
Light	100	14.6	100	8.9	100	6.9	100	9.1
Dark	94 (6)[(c)]	4.7	98 (2)[(c)]	6.9	100	5.9	100	3.8

[(a)] A(rel.) = A_{light}·and A(rel.) = A_{dark}·for the light and dark relaxation phases, respectively; [(b)] $k = k_{light}$ and $k = k_{dark}$ for the light and dark relaxation phases, respectively; [(c)] A_{∞} in the dark relaxation phase

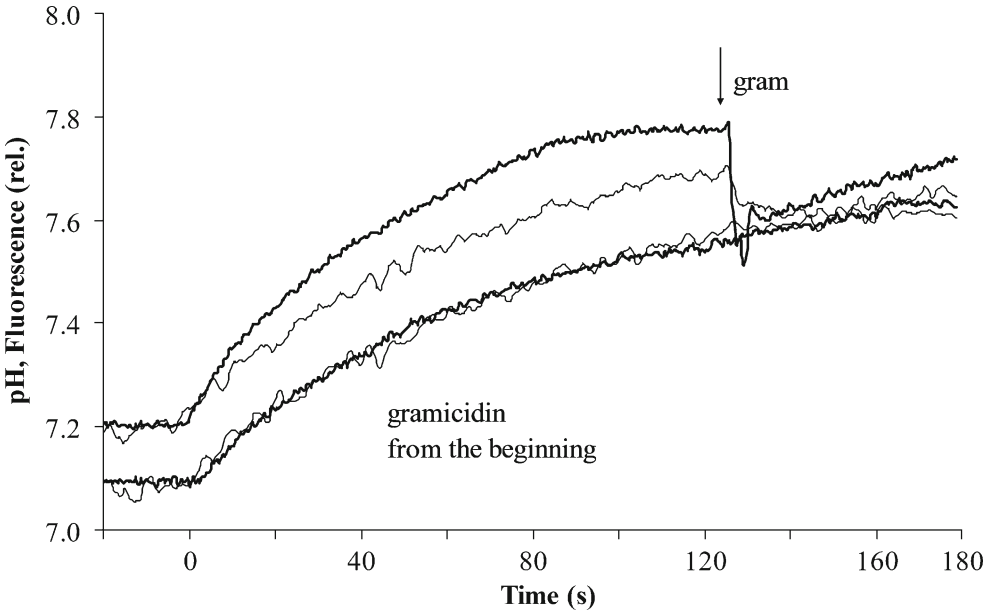

Fig. 7 The relative increase of the pyranine fluorescence (*thick lines*) inside and the change of the pH outside (*thin lines*) the RC/lipid vesicles. The later was measured directly by a pH electrode immersed into the reaction mixture. The fluorescence signal was normalized to the trace of the gramicidin treated signal in order to compare the rates of the changes. 10 μg/ml gramicidin was added from ethanolic solution when indicated

phase was not speeded up, even more it became a little bit smaller (k_{dark} = 3.8 ×10^{-3} s^{-1}). It is inferred that valinomycin does not affect the proton permeability of the membrane noticeably.

Further evidence of transmembrane proton gradient photogeneration is given by the simultaneous measure of inside and outside pH during illumination. In order to monitor the pH changes parallel in- and outside of the vesicles we immersed a pH electrode in the RC mixture and the output signal of the pH meter was connected to one channel of an USB analog/digital converter, while the other channel monitored the signal of the pyranine fluorescence. The typical signal can be seen in Fig. 7 where is shown that both the outside and the inside pH increase under illumination; however, there is a steeper increase in the fluorescence signal indicating more and faster alkalization inside the vesicles. Addition of gramicidin, as it was expected, resulted in a sudden, about ΔpH = 0.3 pH change and since the RC

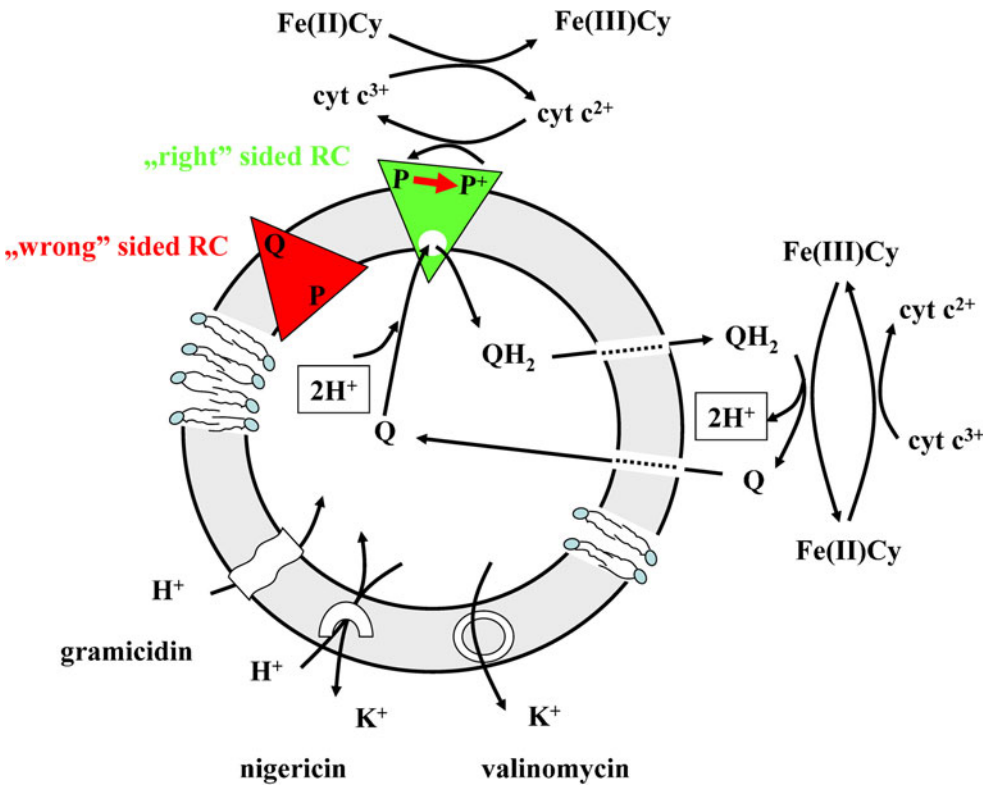

Fig. 8 The scheme of the overall processes, the photochemical generation of delta pH and the effect of the ionophores. The explanations are given in the text

photochemistry is still driven by the light a new equilibrium is created slowly. Finally, if the gramicidin is present from the beginning of the experiment, the inside and outside pH is changing simultaneously with the same rate. These results confirm our model describing the system in terms of equilibrium between proton consumption driven by the photocycle, passive proton wiring across the membrane (and the quinol reoxidation–this latter can be neglected here). Alkalization in both sides of the membrane during the light phase is expected due to the proton membrane permeability, but proton equilibration is slow enough so that pH changes faster inside than outside. After addition of gramicidin to the sample protons are quickly equilibrated across the membrane, so that the difference disappears.

Conclusions

Proteoliposomes were prepared with low proton permeability that were found to be suitable for photogeneration of a transmembrane proton gradient. The main requirements for an enhanced proton sealing ability in our experiments were: a) presence of palmitoyl and oleoyl groups that provide proper physico/chemical nature (microviscosity) of the membrane by the relatively low melting temperature as well as eliminating the hydrophobic mismatch between the hydrophobic thicknesses of the transmembrane α-helices of the RC and the lipid bilayer (Katona et al. 2003); b) presence of cholesterol that modulates the packing of the phospholipid molecules in the lipid bilayer and changes the water content, consequently the distribution of water wires in the membrane. This packing is very important for the proper rigidity, durability and passive permeability. c) presence of PG or PI (both are anionic lipids and are natural constituents of the bacterial membrane), that prevent the attachment of pyranine on the surface of the bilayer. d) use of OG instead of Ch to solubilize the lipids into mixed micelles. Different detergents may also modify the domain formation (structure and distribution) of the membrane.

In the POPC/cholesterol/PI (5:5:1 molar ratio) proteoliposomes with proper donor/acceptor system the RC's photochemistry can generate a trans membrane proton gradient. It is collapsed by detergent TX-100. The kinetics of the photochemical building up of the ΔpH and the passive recovery can be modified with ionophores gramicidin, nigericin and valinomycin and the kinetics of the reoxidation of the reduced quinols. The overall processes, the ΔpH photochemical generation and the effects of the ionophores are summarized in Fig. 8. The experimental arrangement what we designed and presented here provides a useful tool for future studies of the membrane permeabilization by photosynthetic systems which includes the proton conductivity as a complex combination of lipid phase behaviour, domain distribution, protein rearrangement, interaction of redox centers and membrane dynamics.

Acknowledgments This work was supported by the grants from Hungarian (OTKA, T 42680, NKTH/OTKA K-67850), Italian (MTA/CNR, FIRB-MIUR, Cofin–MIUR 2002) and Canadian (NSERC, CFI) founding agencies and from COST action CM0902. The authors wish to thank Dr. Marina Nardulli for the fluorescence microscopy images.

References

Agostiano A, Mavelli F, Milano F, Giotta L, Trotta M, Nagy L et al (2004) pH-sensitive fluorescent dye as probe for proton uptake in photosynthetic reaction centers. Bioelectrochemistry 63(1–2):125–128

Allen JP, Williams JC (1998) Photosynthetic reaction centers. FEBS Lett 438(1–2):5–9

Barlic A, Gutierrez-Aguirre I, Caaveiro JM, Cruz A, Ruiz-Arguello MB, Perez-Gil J et al (2004) Lipid phase coexistence favors membrane insertion of equinatoxin-II, a pore-forming toxin from Actinia equina. J Biol Chem 279(33):34209–34216

Blankenship RE, Madigan TM, Bauer CE (eds) (1995) Anoxygenic photosynthetic bacteria (advances in photosynthesis). Kluwer Academic Publishers, Dordrecht

Brzustowicz MR, Cherezov V, Caffrey M, Stillwell W, Wassall SR (2002) Molecular organization of cholesterol in polyunsaturated membranes: microdomain formation. Biophys J 82(1 Pt 1):285–298

de Almeida RF, Loura LM, Fedorov A, Prieto M (2005) Lipid rafts have different sizes depending on membrane composition: a time-resolved fluorescence resonance energy transfer study. J Mol Biol 346(4):1109–1120

Deamer DW, Harang E (1990) Light-dependent pH gradients are generated in liposomes containing ferrocyanide. Biosystems 24 (1):1–4

Deamer DW, Nichols JW (1989) Proton flux mechanisms in model and biological membranes. J Membr Biol 107(2):91–103

Donohue TJ, Cain BD, Kaplan S (1982) Alteration in the phospholipid composition of Rhodopseudomans sphaeroides and other bacteria induced by Tris. J Bacteriol 152:595–606

Duan L, Qi W, Yan X, He Q, Cui Y, Wang K et al (2009) Proton gradients produced by glucose oxidase microcapsules containing motor F0F1-ATPase for continuous ATP biosynthesis. J Phys Chem B 113(2):395–399

Faxen K, Brzezinski P (2007) The inside pH determines rates of electron and proton transfer in vesicle-reconstituted cytochrome c oxidase. Biochim Biophys Acta 1767(5):381–386. doi:10.1016/j.bbabio.2007.02.023

Filizola M, Wang SX, Weinstein H (2006) Dynamic models of G-protein coupled receptor dimers: indications of asymmetry in the rhodopsin dimer from molecular dynamics simulations in a POPC bilayer. J Comput Aided Mol Des 20(7–8):405–416

Gensure RH, Zeidel ML, Hill WG (2006) Lipid raft components cholesterol and sphingomyelin increase H+/OH- permeability of phosphatidylcholine membranes. Biochem J 398(3):485–495

Gutknecht J (1987) Proton/hydroxide conductance and permeability through phospholipid bilayer membranes. Proc Natl Acad Sci U S A 84(18):6443–6446

Hauska G, Samoray D, Orlich G, Nelson N (1980) Reconstitution of photosynthetic energy conservation. II. Photophosphorylation in liposomes containing photosystem-I reaction center and chloroplast coupling-factor complex. Eur J Biochem 111(2):535–543

Hellingwerf KJ (1987) Reaction centers from Rhodopseudomonas sphaeroides in reconstituted phospholipid vesicles. I. Structural studies. J Bioenerg Biomembr 19(3):203–223

Henriksen J, Rowat AC, Brief E, Hsueh YW, Thewalt JL, Zuckermann MJ et al (2006) Universal behavior of membranes with sterols. Biophys J 90(5):1639–1649

Holoubek A, Vecer J, Sigler K (2007) Monitoring of the proton electrochemical gradient in reconstituted vesicles: quantitative measurements of both transmembrane potential and intravesicular pH by ratiometric fluorescent probes. J Fluoresc 17(2):201–213

Kahya N, Schwille P (2006) How phospholipid-cholesterol interactions modulate lipid lateral diffusion, as revealed by fluorescence correlation spectroscopy. J Fluoresc 16(5):671–678

Kalman L, Gajda T, Sebban P, Maroti P (1997) pH-metric study of reaction centers from photosynthetic bacteria in micellular solutions: protonatable groups equilibrate with the aqueous bulk phase. Biochemistry 36(15):4489–4496

Kano K, Fendler JH (1978) Pyranine as a sensitive pH probe for liposome interiors and surfaces. pH gradients across phospholipid vesicles. Biochim Biophys Acta 509(2):289–299

Katona G, Andreasson U, Landau EM, Andreasson LE, Neutze R (2003) Lipidic cubic phase crystal structure of the photosynthetic reaction centre from Rhodobacter sphaeroides at 2.35A resolution. J Mol Biol 331(3):681–692

Krishnamoorthy I, Krishnamoorthy G (2001) Probing the link between proton transport and water content in lipid membranes. J Phys Chem B 105:1484–1488

Lande MB, Donovan JM, Zeidel ML (1995) The relationship between membrane fluidity and permeabilities to water, solutes, ammonia, and protons. J Gen Physiol 106(1):67–84

Milano F, Gerencser L, Agostiano A, Nagy L, Trotta M, Maroti P (2007) Mechanism of quinol oxidation by ferricenium produced by light excitation in reaction centers of photosynthetic bacteria. J Phys Chem B 111(16):4261–4270

Milano F, Italiano F, Agostiano A, Trotta M (2009) Characterisation of RC-proteoliposomes at different RC/lipid ratios. Photosynth Res 100(2):107–112. doi:10.1007/s11120-009-9423-5

Molenaar D, Crielaard W, Hellingwerf KJ (1988) Characterization of protonmotive force generation in liposomes reconstituted from phosphatidylethanolamine, reaction centers with light-harvesting complexes isolated from Rhodopseudomonas palustris. Biochemistry 27(6):2014–2023. doi:10.1021/bi00406a031

Nagy L, Fodor E, Farkas T, Gedey S, Kecskes A (1999) Lipids effect the charge stabilisation in wild type and mutant reaction centres of photosynthetic bacteria Rhodobacter sphaeroides. Aust J Plant Physiol 25:465–473

Okamura MY, Paddock ML, Graige MS, Feher G (2000) Proton and electron transfer in bacterial reaction centers. Biochim Biophys Acta 1458(1):148–163

Onishi JC, Niederman RA (1982) Rhodopseudomonas sphaeroides membranes: alterations in phospholipid composition in aerobically and phototrophically grown cells. J Bacteriol 149(3):831–839

Osvath S, Maroti P (1997) Coupling of cytochrome and quinone turnovers in the photocycle of reaction centers from the photosynthetic bacterium Rhodobacter sphaeroides. Biophys J 73(2):972–982

Paddock ML, Feher G, Okamura MY (2003) Proton transfer pathways and mechanism in bacterial reaction centers. FEBS Lett 555(1):45–50

Pandit SA, Chiu SW, Jakobsson E, Grama A, Scott HL (2007) Cholesterol surrogates: a comparison of cholesterol and 16:0 ceramide in POPC bilayers. Biophys J 92(3):920–927

Petrova IO, Kurashov VN, Semenov AY, Mamedov MD (2011) Manganese-depleted/reconstituted photosystem II core complexes in solution and liposomes. J Photochem Photobiol B 104(1–2):372–376

Pilotelle-Bunner A, Beaunier P, Tandori J, Maroti P, Clarke RJ, Sebban P (2009) The local electric field within phospholipid membranes modulates the charge transfer reactions in reaction centres. Biochim Biophys Acta 1787(8):1039–1049

Riegler J, Mohwald H (1986) Elastic interactions of photosynthetic reaction center proteins affecting phase transitions and protein distributions. Biophys J 49(6):1111–1118

Sebban P, Maroti P, Hanson DK (1995) Electron and proton transfer to the quinones in bacterial photosynthetic reaction centers: insight from combined approaches of molecular genetics and biophysics. Biochimie 77(7–8):677–694

Shinkarev VP, Wraight CA (1993) Electron and proton transfer in the acceptor quinone complex of reaction centres of phototrophic bacteria. In: Deisenhofer J, Norris JR (eds) The photosynthetic reaction center. Academic, San Diego, pp 193–255

Steiner S, Sejka GA, Conti SF, Gest H, Lester RL (1970) Modification of membrane composition in growing photosynthetic bacteria. Biochim Biophys Acta 203(3):571–574

Tandori J, Nagy L, Puskás Á, Droppa M, Horváth G, Maróti P (1995) The IleL229 → Met mutation impairs the quinone binding to the QB-pocket in reaction centers of Rhodobacter sphaeroides. Photosynth Res 45(2):135–146

Telford JE, Kilbride SM, Davey GP (2010) Decylubiquinone increases mitochondrial function in synaptosomes. J Biol Chem 285 (12):8639–8645

Thewalt JL, Bloom M (1992) Phosphatidylcholine: cholesterol phase diagrams. Biophys J 63(4):1176–1181

Trotta M, Milano F, Nagy L, Agostiano A (2002) Response of membrane protein to the environment: the case of photosynthetic reaction centre. Mater Sci Eng C 22(2):263–267

van Rotterdam BJ, Westerhoff HV, Visschers RW, Bloch DA, Hellingwerf KJ, Jones MR et al (2001) Pumping capacity of bacterial reaction centers and backpressure regulation of energy transduction. Eur J Biochem 268(4):958–970

Wardak A, Brodowski R, Krupa Z, Gruszecki WI (2000) Effect of light-harvesting complex II on ion transport across model lipid membranes. J Photochem Photobiol B 56(1):12–18

Wiedenmann A, Dimroth P, von Ballmoos C (2008) Deltapsi and DeltapH are equivalent driving forces for proton transport through isolated F(0) complexes of ATP synthases. Biochim Biophys Acta 1777(10):1301–1310

Wood BJB, Nichols BW, James AT (1965) The lipids and fatty acid metabolism of photosynthetic bacteria. Biochim Biophys Acta 106:261–273

Wraight CA (2004) Proton and electron transfer in the acceptor quinone complex of photosynthetic reaction centers from Rhodobacter sphaeroides. Front Biosci 9:309–337

Yang Z, Su X, Wu F, Gong Y, Kuang T (2005) Photochemical activities of plant photosystem I particles reconstituted into phosphatidylglycerol liposomes. J Photochem Photobiol B 78(2):125–134